

**Effects of color reconnection on hadron flavor observables**Christian Bierlich<sup>\*</sup> and Jesper Roy Christiansen<sup>†</sup>*Department of Astronomy and Theoretical Physics, Lund University, Sölvegatan 14A, SE-223 62 Lund, Sweden*

(Received 10 September 2015; published 5 November 2015)

We present a series of observables for soft inclusive physics, and utilize them for comparison between two recently developed color reconnection models: the new color reconnection model in Pythia and the DIPSY rope hadronization model. The observables are ratios of identified hadron yields as a function of the final-state activity, as measured by the charged multiplicity. Since both considered models have a nontrivial dependence on the final-state activity, the above observables serve as excellent probes to test the effect of these models. Both models show a clear baryon enhancement with increasing multiplicity, while only the DIPSY rope model leads to a strangeness enhancement. Flowlike patterns, previously found to be connected to color reconnection models, are investigated for the new models. Only Pythia shows a  $p_{\perp}$ -dependent enhancement of the  $\Lambda/K$  ratio as the final-state activity increases, with the enhancement being largest in the mid- $p_{\perp}$  region.

DOI: 10.1103/PhysRevD.92.094010

PACS numbers: 12.38.-t, 13.85.Ni

**I. INTRODUCTION**

The first run of the LHC has provided a large number of measurements probing both soft and hard QCD, and thereby a large number of tests for the Monte Carlo event generators. Even though the overall performance of the event generators has been quite good, there are still some phenomena that are insufficiently understood [1]. One of the more intriguing soft QCD deviations is the observed enhancement of  $\Lambda$  production [2,3]. No model has been simultaneously able to describe the identified hadron spectra at both the LEP and LHC. This has led to the development of several phenomenological models [4–6], partly aimed to address this problem. With the planned low pileup runs at the beginning of the second LHC run, it is now an ideal time to test these models further, and thereby probe the physical origin of the  $\Lambda$  enhancement. In this study we consider two of the models: the new color reconnection (CR) model in the Pythia event generator [5,7] and the color rope model in the DIPSY event generator [4,8,9]. The models have previously been compared to  $pp$  data at  $\sqrt{s}$  of 200, 900 and 7000 GeV. In this paper new possible observables to test the models are suggested, and predictions are made for collisions at  $\sqrt{s} = 13$  TeV. The observables are not model dependent, and can be used for constraining predictions from other models of soft inclusive physics. Both considered color reconnection models are built upon the Lund model for string hadronization [10]. Nonperturbative differences can therefore be ascribed to differences in the new phenomenological ideas.

One of the key ideas for the two models in question is *jet universality*. Stated in terms of the string model, it

essentially means that fragmentation of a string does not depend on how the string is formed. Free strings at both lepton and hadron colliders should thus hadronize in a similar fashion. Fragmentation parameters are therefore tuned in the clean  $e^+e^- \rightarrow Z \rightarrow q\bar{q}$  environment, and then directly applied to hadron colliders. Any discrepancy has to be due to physical phenomena not active at lepton colliders. For all the models attempting to describe the  $\Lambda$  enhancement, the enhancement is linked to the increased density of quarks and gluons in the final state at hadron colliders [11]. It would therefore be of natural interest to measure the  $\Lambda$  enhancement as a function of this density. The quark-gluon density is experimentally ill defined, however, and we suggest using the number of charged tracks in the forward region as a measure of final-state activity. A similar idea for using the hyperon-to-meson ratio to search for indications of a mini-QGP was suggested in Ref. [12]. We suggest ratios that allow for separation of strangeness enhancement from baryon enhancement, which both could be present in the hyperon-to-meson ratio.

Another puzzling observation is the indication of collective effects in high-multiplicity  $pp$  collisions [13,14], often interpreted as the presence of flow. These effects were only expected in the dense medium of heavy ion collisions, where the pressure gradients give rise to flow effects. A study of the models for  $pp$  collisions showed that CR generated similar effects even without the introduction of a thermalized medium [15]. We therefore consider one of the standard observables in heavy ion physics, that of identified particle ratios as a function of  $p_{\perp}$ , separated into bins of centrality, and compare the model predictions for  $pp$  collisions. Since centrality is not experimentally well defined in  $pp$  collisions, the number of charged tracks in the forward region is used as a measure of activity.

The outline of the paper is as follows. In Sec. II we briefly recap the most important features of the two models

<sup>\*</sup>christian.bierlich@thep.lu.se<sup>†</sup>jesper.christiansen@thep.lu.se

considered. Comparison to existing  $e^+e^-$  data at  $\sqrt{s} = 91.2$  GeV, and  $pp$  data at  $\sqrt{s}$  of 200 GeV and 7 TeV, is shown in Sec. III. The event selection and tuning for 13 TeV is described in Sec. IV. In Sec. V, the predictions at  $\sqrt{s} = 13$  TeV, for the second run of the LHC, are presented. Finally, in Sec. VI, we summarize and present an outlook.

## II. THE MODELS

Both models for color reconnection are built upon the Lund string model for hadronization. In this model, outgoing partons are connected with stringlike color fields, which fragment into hadrons when moving apart. The model contains two main parameters relevant to this study, which determine the suppression of strange quarks and of diquarks (giving baryons) in the breakups. Assuming jet universality, these parameters are tuned to LEP data.

Baryons can in addition be created around string junctions, which can arise as a consequence of color reconnection. Consider the simple configuration of two  $q\bar{q}$  dipoles in Fig. 1, which for example could have originated from a decay of two  $W$ -bosons in a LEP environment, as described in Ref. [16]. What essentially could be described as a quadrupole configuration is instead described as either the original (on top) or the left configuration in Fig. 1. Without CR only the original configuration is considered. Extending this type of color reconnection to hadron colliders has been shown [17] to be a necessary condition to describe the rising of  $\langle p_{\perp} \rangle (N_{\text{ch}})$  distributions. The QCD  $\varepsilon$ -tensor gives rise to the rightmost configuration, containing two junction connections, depicted as empty circles. Since such junctions constitute protobaryons, in the same way string segments constitute protomesons, they become an additional source of baryons.

### A. Color reconnection in Pythia

The new CR model in Pythia is situated just prior to the hadronization. It takes the leading-color ( $N_c \rightarrow \infty$ ) strings and transform them to a different color configuration based on three principles: first, the SU(3) color rules from QCD determine if two strings are color compatible (e.g. there is only a  $1/9$  probability that the top configuration of Fig. 1

can transform to the left configuration purely from color considerations); secondly, a simplistic space-time picture to check causal contact between the strings; and finally the  $\lambda$  measure [18] [which is a string-length measure,  $\lambda = \sum_i \log(1 + m_i^2/(2m_0^2))$  where the sum goes over all dipoles,  $m_i$  is the invariant mass of the dipole and  $m_0$  is a parameter] to decide whether a possible reconnection is actually favored. Since the model relies purely on the outgoing partons, it is in principle applicable to any type of collision. So far it has only been tested for  $pp$  [5] and  $ee$  collisions [19]. The main extension compared to the other CR models in Pythia is the introduction of reconnections that form junction structures. From a pure color consideration the probability to form a junction topology is three times larger than an ordinary reconnection. The junction will introduce additional strings, however, and it is therefore often disfavored due to a larger  $\lambda$  measure. Given the close connection between junctions and baryons, the new model predicts a baryon enhancement. It was shown to be able to simultaneously describe the  $\Lambda$  production for both LEP and LHC experiments, which neither of the earlier Pythia tunes have been able to.

The new CR model essentially contains two new parameters: a parameter that constrains the overall strength of the CR, and a parameter that controls the baryon enhancement. Both of these parameters were tuned to data [3,20] from the LHC experiments at 7 TeV.

### B. Rope hadronization in DIPSY

Rope hadronization [21] is an umbrella term for QCD inspired models, which include interactions between strings. From previous attempts to include this effect in Monte Carlo generators [22], it is well known that strange and baryonic content will rise in very dense events.

A model introducing rope hadronization was recently developed and implemented in the event generator DIPSY [4]. Along with a final-state swing, the model introduces local calculation of string density, and corrects the evolution of the final-state parton shower and hadronization based on this local density.

The model is based upon the idea [21] that when several parton pairs are next to each other in geometric space, they

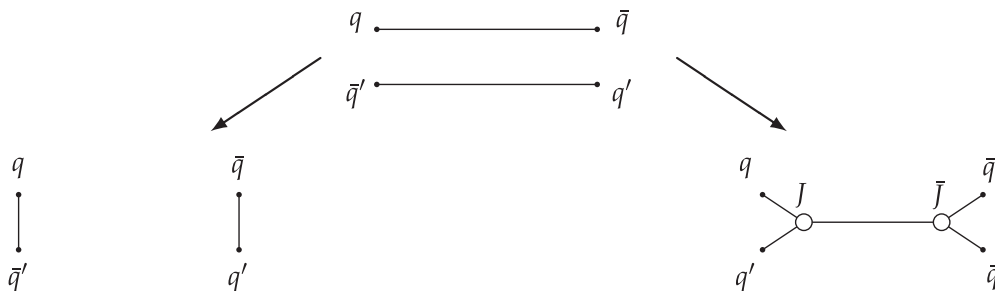


FIG. 1. Sketch of how two  $q\bar{q}$  dipoles (top) can be reconnected to different color topologies (left and right). The right connection gives rise to a double junction, which in turn will produce baryons. Notice that the placement of the pairs differs in the junction figure.

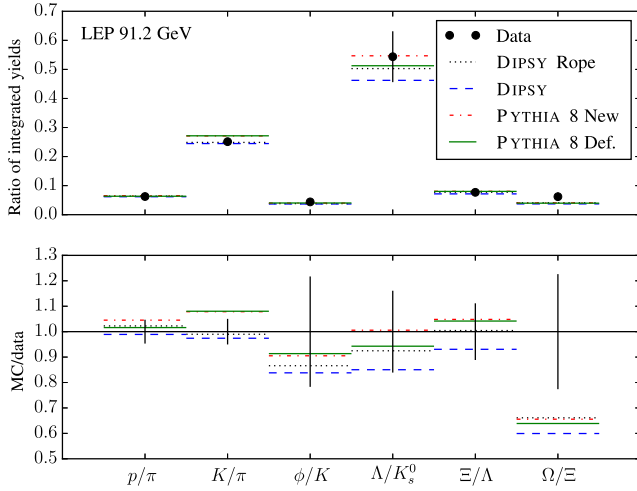


FIG. 2 (color online). Comparison to  $e^+e^-$  at 91.2 GeV from ALEPH, SLD and PDG.

can act together coherently to form a color rope. Each string is treated as a flux tube with a fixed radius, and the amount of overlap between strings, in impact parameter space and rapidity, can be directly calculated.

If such an overlap is found to exist, it can have different effects, determined by SU(3) color rules. The overlapping strings can end up in a color singlet configuration. This is handled by a final-state swing that reconnects color dipoles, in the final-state parton shower as the transformation from the top to the bottom left configuration in Fig. 1. In all other cases, the strings end up forming a rope. This is hadronized with a higher effective string tension, reflecting the fact that more energy is available for the fragmentation, in accordance with results from lattice QCD [23]. In some cases, the strings forming the rope end up in a junction structure. In such cases the junction pair is handled using a simple approach, where the two junctions collapse to either two diquarks or two quarks, with a probability controlled by a tuneable parameter. The resulting strings are then hadronized with the appropriate effective string tension.

An increased string tension results in more strange quarks and diquarks produced in string breakups. Since the effect increases with the density of quarks and gluons in the final state, the expected outcome is more baryons and strangeness among the resulting hadrons. The model includes two free parameters; the string radius and the probability for a junction to resolve to diquarks. Both are tuned to LHC data [3] at 7 TeV.

### III. COMPARISON TO DATA

The models perform as intended when comparing to existing data. Ratios of baryons to mesons are enhanced for both models, whereas ratios of particles with strange quark content are enhanced only in the DIPSY rope model. Comparisons are done to ratios of integrated yields of identified particles, using the analyses published through the Rivet [24] framework. The raw results from comparing the Monte Carlo to data using Rivet are integrated to give Figs. 2 and 3, using Matplotlib [25]. Error estimates are conservative, as they assume the error of all bins is fully correlated.

In Fig. 2, a comparison to LEP data [26–28] is seen. Two conclusions can be drawn from this figure. First of all, these are the data the original string model is tuned to. The fact that the Monte Carlo is so well aligned with data is thus not an indication that the string model predicts all these ratios so well, but rather that the parameters of the model are tuned to these data. The exception here is the  $\Omega$  baryon [29], reflected in the  $\Omega/\Xi$  ratio, which lies below the observed value. However, the experimental statistical uncertainty is large for this ratio.

The other conclusion, which is the most relevant for this article, is that only small effects at LEP data are observed. The  $\Lambda/K$  ratio increases by about 10% for both the DIPSY rope model and the new CR model in Pythia (over their respective default models), but all models stay within the experimental uncertainty. The overall low variance is

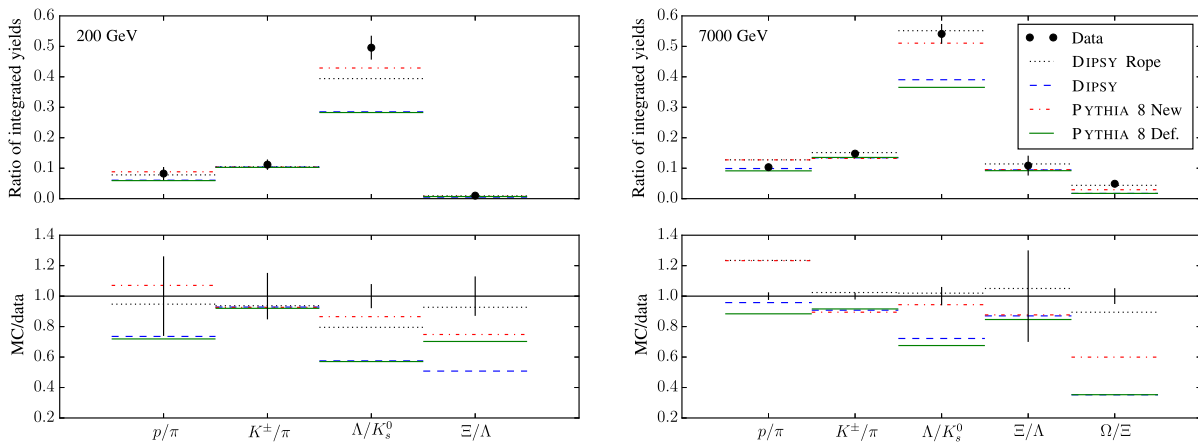


FIG. 3 (color online). Comparison to  $pp$  data at 200 GeV from STAR (left) and at 7 TeV from ALICE and CMS (right).

exactly what is expected, due to the low final-state activity at the LEP.

In Fig. 3 comparison to STAR data [30–32] at 200 GeV indicated that the description of the baryon-to-meson ratios improves with both models, while the description of the  $\Xi/\Lambda$  ratio only improves with the DIPSY rope model. The change in the  $K^\pm/\pi$  ratio is not visible on this scale for this energy.

Comparison to 7 TeV data from ALICE [33,34] and CMS [3] confirms that the description improves, even for the  $\Omega/\Xi$  ratio. The description of the  $p/\pi$  ratio is seen to be somewhat worse with the new models. This could either have a mundane explanation originating in the fact that the very low- $p_\perp$  area of the individual distributions (which contains most of the multiplicity) is not fully understood, or have further reaching consequences. We point to the measurements suggested in the next section of this paper to shed light on this issue.

#### IV. TUNING AND EVENT SELECTION

Before studying exclusive observables at 13 TeV, it is necessary to verify that the baselines for the two models agree reasonable well. Normally this is achieved by tuning the models to the available data. Data at  $\sqrt{s} = 13$  TeV are, however, not yet published in a state where event generators can be tuned to it, so the DIPSY model was instead tuned to the Pythia predictions for  $dN_{\text{ch}}/d\eta$ ,  $\langle p_\perp \rangle(N_{\text{ch}})$  and the

multiplicity distribution. Both models will eventually have to be retuned, when more data, in a suitable format for tuning, become available. Only small effects are expected from the retuning, first due to fragmentation mainly being determined from LEP data, and secondly since the already presented results at 13 TeV show a good agreement between the Monash tune and the data [35,36]. The full list of all parameters changed from their default values is included in an appendix.

An event and particle selection was implemented to mimic a possible experimental setup. Each particle is required to have  $p_\perp > 0.15$  GeV. Two different  $\eta$  regions are used: a forward region ( $2 < |\eta| < 5$ ) to measure the activity, and a central region ( $|\eta| < 1$ ) to measure the identified hadron yields. The reason for the split is to avoid any potential bias, which otherwise happens at low  $N_{\text{ch}}$ , in particular for ratios involving both charged and noncharged hadrons. Since DIPSY does not have a model for diffraction, only non-diffractive events are considered for both models. To reflect this in the event selection, only events with at least six forward charged particles are considered.

All particles with  $c\tau > 10$  mm are treated as stable. In practice this means that  $\pi^\pm$ ,  $K$ ,  $\Lambda$ ,  $\Xi$  and  $\Omega$  are all stable whereas  $\phi$  (which decays strongly) is not. This introduces some double counting in the  $\phi/K$ -ratio, where a  $\phi$  can potentially be counted in the numerator and its decay products in the denominator.

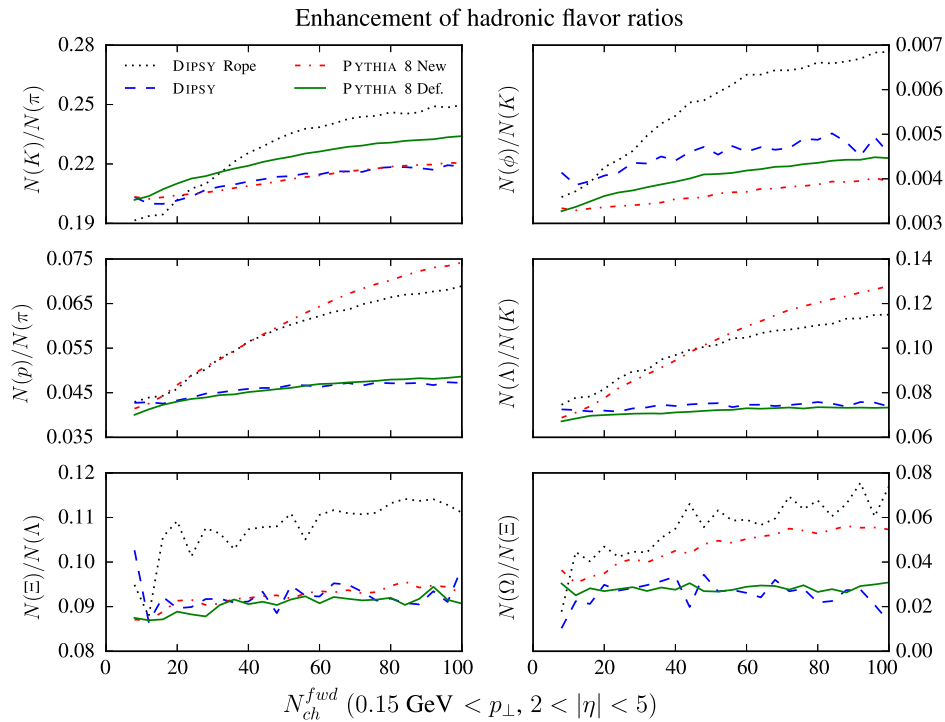


FIG. 4 (color online). Ratios of identified hadrons as functions of  $N_{\text{ch}}^{\text{fwd}}$  at  $\sqrt{s} = 13$  TeV. The top row shows meson ratios with the numerator having one more strange quark than the denominator. The middle row shows baryon-to-meson ratios, with same amount of strange quarks. The bottom row shows baryon ratios with the numerator having one more strange quark than the denominator. Note that the vertical axis differs between the figures and that zero is suppressed.



## V. PREDICTIONS FOR 13 TEV

Differences between the color reconnection models are best determined using observables controlled by hadronization effects. Ratios of identified particles are exactly such an observable, since particle species production is determined by the quark and diquark content in string breaks. In the first part of this section, ratios of identified particles are shown as a function of  $N_{\text{ch}}$  in the forward region, as a measure of event activity. Then flowlike effects are considered, by showing  $(\Lambda/K)(p_{\perp})$  in four different bins of  $N_{\text{ch}}$  in the forward region.

### A. Particle ratios

Ratios of hadrons with different strange and baryon numbers as a function of event activity, measured as functions of  $N_{\text{ch}}^{\text{fwd}}$ , are shown in Fig. 4. The strangeness enhancement in meson production is probed by the  $K/\pi$  and  $\phi/K$  ratios, for which the numerator always contains one more strange quark than the denominator. As expected, only the DIPSY rope model shows an enhancement relative to the baseline, since it contains a strangeness enhancement. The new Pythia CR model lies slightly below the baseline. This can be explained by phase-space constraints for low invariant-mass strings, which the new model produces more of. It should be recalled that both the new as well as the old models are capable of describing the total  $K_s^0$  yield at 7 TeV. Thus, the limited effects in this ratio are somewhat expected. The  $\phi/K$  ratio shows more

promise as a means to distinguish between the two models, since the DIPSY model shows a larger enhancement. It is, however, more experimentally challenging.

The baryon enhancement is tested for both hadrons containing zero or one strange quark,  $p/\pi$  and  $\Lambda/K$ . For both ratios, and both models, clear enhancements are expected and seen. For the  $\Lambda/K$  ratio both models agree quite well, which is not surprising, given that both models are tuned to describe the inclusive  $\Lambda/K$  distributions at 7 TeV. A similar picture is seen for the  $p/\pi$  ratio, indicating similar predictions for the baryon enhancement from both the models.

The multistrange baryon enhancement is tested in the same way as the strange-meson enhancement by considering the ratios  $\Xi/\Lambda$  and  $\Omega/\Xi$ . The large variations at low multiplicity for both distributions are due to statistical fluctuations. For  $\Xi/\Lambda$  the DIPSY rope model shows a clear enhancement as opposed to the new Pythia CR model. The  $\Lambda/p$  ratio is not shown, but the enhancement is similar to the enhancement of  $\Xi/\Lambda$ . An enhancement is seen for both models in the  $\Omega/\Xi$ , with the enhancement factor being around 2.5 for the DIPSY rope model in the highest multiplicity bins. This is larger than any of the other enhancements seen. The enhancement for the new Pythia CR model is somewhat surprising, as the increased junction production should be equal for both  $\Xi$  and  $\Omega$ . The production of  $\Omega$  in the standard Pythia fragmentation is, however, significantly suppressed, as the production of  $ss$  diquarks is disfavored. This suppression is not present in

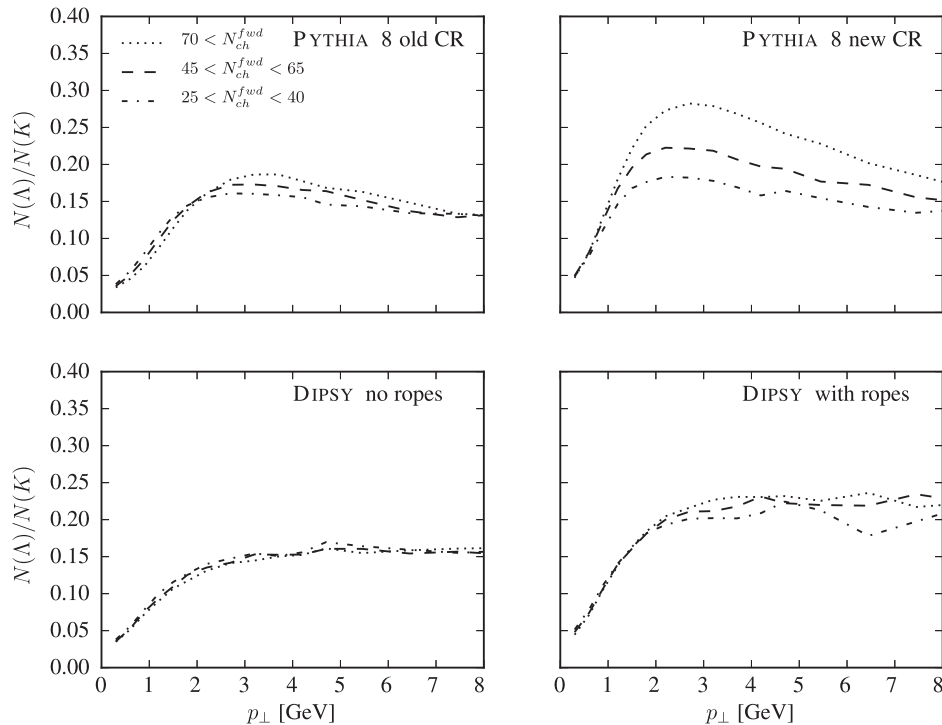


FIG. 5. Ratio of  $\Lambda/K$  as a function of  $p_{\perp}$  in three bins of  $N_{\text{ch}}^{\text{fwd}}$ . In the right column the new color reconnection models are shown, and in the left column the old ones.

the junction handling, since it takes two already formed quarks and combines into a diquark. The enhancement in the new Pythia model should therefore not be interpreted as a “real” strangeness enhancement, but more as an absence of suppression of  $ss$  diquarks. For the DIPSY model the above effect is also present, but there is an additional enhancement of strangeness and diquarks. It should be noted that the  $\Omega$  baseline from LEP is not that well constrained, due to a large experimental uncertainty, and the model predictions are below the actual measurements. A measurement of  $(\Omega/\Xi)(N_{\text{ch}})$  would cast light on whether an actual activity-based enhancement takes place.

Increased hyperon production in high activity  $pp$  events has previously been associated with production of a mini-QGP [12]. The hyperon-to-pion ratio is only indirectly shown in Fig. 4, but the rise is similar to the one predicted by mini-QGP. The new models therefore provide an alternative explanation, if such an enhancement is observed.

### B. Flowlike effects

The  $\Lambda/K$  ratio as a function of  $p_{\perp}$  for different  $N_{\text{ch}}^{\text{fwd}}$  ranges is shown in Fig. 5. The two models show different behaviors for the different multiplicity ranges: the DIPSY rope model only gives a small enhancement ( $\sim 10\%$  at maximum) between the lowest and highest multiplicity regions. Even though the differential enhancement is generally below 10%, the enhancement of the ratio of integrated yields is about 20%, which is in good agreement with Fig. 4. It should be noted that the DIPSY model is inadequate in describing the high  $p_{\perp}$  tails ( $p_{\perp} > \sim 4$  GeV). This was observed for 900 GeV and 7 TeV in Ref. [4].

The new Pythia CR model shows a clear change in  $p_{\perp}$  with increasing multiplicity. The enhancement is largest in the mid- $p_{\perp}$  region ( $p_{\perp} \sim 2\text{--}6$  GeV), leading to a “peak” structure. This structure looks qualitatively similar to what is observed in  $PbPb$  and  $pPb$  collisions [37,38]. The peak also moves towards larger  $p_{\perp}$  with increased multiplicity, an effect normally attributed to radial flow in heavy ion collisions [39]. That the new CR model predicts a qualitatively similar effect in  $pp$  collisions is quite intriguing and strengthens the hint at a potential connection between flow and CR effects already observed [15].

## VI. CONCLUSIONS

A series of new model-independent observables, well suited for distinguishing between different physical models for soft inclusive physics, is suggested. The observables are ratios of identified hadrons measured as a function of event activity, with the identified hadrons chosen such that a distinction is made between baryon-only, strangeness-only

and baryon-and-strangeness enhancement. Measurement of these observables at present and future energies at  $pp$  colliders is encouraged, as they can serve as constraints on any soft physics model aiming to explain low-multiplicity and minimum bias data simultaneously.

The observables are, in this article, used to separate two new CR models. The new CR model in Pythia only contains a baryon enhancement with increasing multiplicity, while the DIPSY rope models contain both a baryon and a strangeness enhancement. The multistrange hyperon ratios, as well as the  $\phi/K$  ratio, provide clear observables for distinguishing between the two models. It should be mentioned that this is already possible to observe in inclusive measurements, but the separation into different multiplicity regions highlights the enhancement.

Both new models are based on interactions between strings in the hadronization phase, and confirmation of the common predictions made by the two models is a direct hint that color reconnections among strings are of physical importance. Both baseline models show almost no dependency on multiplicity for the identified hadron yield ratios. Therefore, any observed dependency would provide a clearer indication that the old models miss a feature, better than an inclusive measurement alone could provide. We therefore strongly suggest that these observables should be measured at the LHC experiments. In this paper we only studied the effects at a center-of-mass energy of 13 TeV, but the effects should also be visible in the already collected data at 7 TeV.

We have also shown that one of the CR models predicts effects similar to those normally attributed to radial flow in heavy ion collisions. This is in agreement with earlier indications that also hint at a connection between the two phenomena. It should however be recalled that neither of the models provides a satisfactory description of the individual  $p_{\perp}$  spectra for the identified hadrons. And before these are fully understood, claims of connections between flow and CR may be premature.

## ACKNOWLEDGMENTS

We thank Leif Lönnblad and Torbjörn Sjöstrand for useful discussions and comments. Work was supported in part by the MCnetITN FP7 Marie Curie Initial Training Network, Grant No. PITN-GA-2012-315877, and the Swedish Research Council, Grant No. 621-2013-4287.

## APPENDIX: MODEL PARAMETERS

A complete list of all the parameters that differ from their default values for the considered models. Hadronization model parameters are found in Table I, Pythia parameters in Table II and DIPSY parameters in Tables III and IV.

TABLE I. Table of parameters of the string hadronization model, which differs from Monash tune [35] default values. The changed parameters have been returned to LEP and SLD data, cf. Fig. 2.

Fragmentation parameter	Pythia default	Pythia new	DIPSY	DIPSY rope
StringPT:sigma	0.335	0.335	0.32	0.31
StringZ:aLund	0.68	0.36	0.30	0.41
StringZ:bLund	0.98	0.56	0.36	0.37
StringFlav:probQQtoQ	0.081	0.078	0.082	0.073
StringFlav:ProbStoUD	0.217	0.22	0.22	0.21
StringFlav:probQQ1toQQ0join	0.5	0.0275	...	...
	0.7	0.0275	...	...
	0.9	0.0275	...	...
	1.0	0.0275	...	...

TABLE II. The new Pythia CR model introduces a number of new parameters, and requires retuning of a few old ones, besides hadronization. The details of the retuning can be found in Ref. [5].

Pythia parameter	Default	New
MultiPartonInteractions:pT0Ref	2.28	2.15
BeamRemnants:remnantMode	0	1
BeamRemnants:saturation	...	5
ColourReconnection:mode	0	1
ColourReconnection:allowDoubleJunRem	on	off
ColourReconnection:m0	...	0.3
ColourReconnection:allowJunctions	...	on
ColourReconnection:junctionCorrection	...	1.2
ColourReconnection:timeDilationMode	...	2
ColourReconnection:timeDilationPar	...	0.18

TABLE III. The DIPSY rope model introduces three extra parameters, which are fixed using  $pp$  data from LHC. See Ref. [4] for the meaning of the parameters.

DIPSY parameter	Default	Rope
FragmentationScheme	default	dipole
StringR0	...	0.773
Stringm0	...	0.113
BetaPopcorn	...	0.2

TABLE IV. The DIPSY initial-state model needs retuning at each energy to reproduce total charged multiplicity. See Ref. [9] for the meaning of the parameters.

Energy	$pp$ 200 GeV		$pp$ 7 TeV		$pp$ 13 TeV	
	Default	Rope	Default	Rope	Default	Rope
LambdaQCD	0.29	0.26	0.17	0.25	0.29	0.27
RMax	2.32	3.34	3.23	2.90	1.05	3.39
PMinusOrdering	1.05	0.98	1.24	0.67	0.31	0.75
PTScale	0.70	0.92	1.60	1.65	1.28	1.35

- [1] A. De Roeck, *Phys. Scr.* **T158**, 014001 (2013).
- [2] K. Aamodt *et al.* (ALICE Collaboration), *Eur. Phys. J. C* **71**, 1594 (2011).
- [3] V. Khachatryan *et al.* (CMS Collaboration), *J. High Energy Phys.* **05** (2011) 064.
- [4] C. Bierlich, G. Gustafson, L. Lönnblad, and A. Tarasov, *J. High Energy Phys.* **03** (2015) 148.
- [5] J. R. Christiansen and P. Z. Skands, *J. High Energy Phys.* **08** (2015) 003.
- [6] T. Pierog, I. Karpenko, J. Katzy, E. Yatsenko, and K. Werner, *Phys. Rev. C* **92**, 034906 (2015).
- [7] T. Sjöstrand, S. Ask, J. R. Christiansen, R. Corke, N. Desai, P. Ilten, S. Mrenna, S. Prestel, C. O. Rasmussen, and P. Z. Skands, *Comput. Phys. Commun.* **191**, 159 (2015).
- [8] E. Avsar, G. Gustafson, and L. Lönnblad, *J. High Energy Phys.* **07** (2005) 062.
- [9] C. Flensburg, G. Gustafson, and L. Lönnblad, *J. High Energy Phys.* **08** (2011) 103.
- [10] B. Andersson, G. Gustafson, G. Ingelman, and T. Sjöstrand, *Phys. Rep.* **97**, 31 (1983).
- [11] This is sometimes also referred to as string density, color density, or energy density.
- [12] V. Topor Pop, M. Gyulassy, J. Barrette, C. Gale, and A. Warburton, *Phys. Rev. C* **86**, 044902 (2012).
- [13] A. Kisiel, *Phys. Rev. C* **84**, 044913 (2011).
- [14] V. Khachatryan *et al.* (CMS Collaboration), *J. High Energy Phys.* **09** (2010) 091.
- [15] A. Ortiz Velasquez, P. Christiansen, E. Cuautle Flores, I. Maldonado Cervantes, and G. Paic, *Phys. Rev. Lett.* **111**, 042001 (2013).
- [16] T. Sjöstrand and V. A. Khoze, *Z. Phys. C* **62**, 281 (1994).
- [17] T. Sjöstrand and M. van Zijl, *Phys. Rev. D* **36**, 2019 (1987).
- [18] B. Andersson, *The Lund Model*, Camb. Monogr. Part. Phys. Nucl. Phys. Cosmol. (Cambridge University Press, Cambridge, 1997).
- [19] J. R. Christiansen and T. Sjöstrand, *Eur. Phys. J. C* **75**, 441 (2015).
- [20] G. Aad *et al.* (ATLAS Collaboration), *New J. Phys.* **13**, 053033 (2011).
- [21] T. S. Biro, H. B. Nielsen, and J. Knoll, *Nucl. Phys.* **B245**, 449 (1984).
- [22] H. Sorge, M. Berenguer, H. Stoecker, and W. Greiner, *Phys. Lett. B* **289**, 6 (1992).
- [23] G. S. Bali, *Phys. Rev. D* **62**, 114503 (2000).
- [24] A. Buckley, J. Butterworth, D. Grellscheid, H. Hoeth, L. Lönnblad, J. Monk, H. Schulz, and F. Siegert, *Comput. Phys. Commun.* **184**, 2803 (2013).
- [25] J. D. Hunter, *Comput. Sci. Eng.* **9**, 90 (2007).
- [26] R. Barate *et al.* (ALEPH Collaboration), *Phys. Rep.* **294**, 1 (1998).
- [27] K. Abe *et al.* (SLD Collaboration), *Phys. Rev. D* **69**, 072003 (2004).
- [28] C. Amsler *et al.* (Particle Data Group), *Phys. Lett. B* **667**, 1 (2008).
- [29] We denote a particle and its antiparticle with just a single letter such that e.g.  $p$  means both proton and antiproton. Special cases are  $\pi$  which denotes  $\pi^+\pi^-$ ,  $K$  which denotes  $K^+K^-K_s^0K_L^0$  and  $\Xi$  which denotes  $\Xi^+\Xi^-$ .
- [30] B. I. Abelev *et al.* (STAR Collaboration), *Phys. Rev. C* **79**, 034909 (2009).
- [31] B. I. Abelev *et al.* (STAR Collaboration), *Phys. Rev. C* **75**, 064901 (2007).
- [32] J. Adams *et al.* (STAR Collaboration), *Phys. Lett. B* **637**, 161 (2006).
- [33] J. Adam *et al.* (ALICE Collaboration), *Eur. Phys. J. C* **75**, 226 (2015).
- [34] B. Abelev *et al.* (ALICE Collaboration), *Phys. Lett. B* **712**, 309 (2012).
- [35] ATLAS Collaboration, Reports No. ATLAS-CONF-2015-028 and No. ATLAS-COM-CONF-2015-046, 2015.
- [36] ATLAS Collaboration, Report No. ATL-PHYS-PUB-2015-019, 2015.
- [37] B. B. Abelev *et al.* (ALICE Collaboration), *Phys. Rev. Lett.* **111**, 222301 (2013).
- [38] B. B. Abelev *et al.* (ALICE Collaboration), *Phys. Lett. B* **728**, 25 (2014).
- [39] R. Fries and B. Müller, *Eur. Phys. J. C* **34**, S279 (2004).